Available online at www.sciencedirect.com
SCIENCE DIRECT®
Sensors and Actuators A 112 (2004) 203–210
SENSORS AND ACTUATORS A PHYSICAL
www.elsevier.com/locate/sna

Quartz crystal microbalance with rigid mass partially attached on electrode surfaces

F. Lu [a], H.P. Lee [a,b,*], S.P. Lim [a]

[a] *Department of Mechanical Engineering, National University of Singapore, 9 Engineering Drive 1, Singapore 117576, Singapore*
[b] *Institute of High Performance Computing, 1 Science Park Road, #01-01 The Capricorn, Singapore Science Park II, Singapore 117528, Singapore*

Received 14 May 2003; received in revised form 8 January 2004; accepted 16 January 2004

Abstract

Quartz crystal microbalance (QCM) vibrating in thickness shear mode is used to detect the mass changes of the layer deposited on its surface. In this paper, an AT-cut quartz crystal microbalance with partial mass absorption on its electrode surface is modeled with Mindlin's theory. The effect of position and percentage of covering area of the mass absorption is studied. The numerical simulation results show that QCM with larger electrode size is less sensitive to the percentage of covering area, and QCM with smaller electrode thickness is less sensitive to the position attachment of the mass absorption on its surface.

Keywords: Sensing; Quartz; Quartz crystal microbalance (QCM)

1. Introduction

Quartz crystal microbalance (QCM) is used to detect the micro mass changes and physical properties of thin layers deposited on the crystal surfaces [1–4]. The active element of a QCM is a thin AT-cut quartz crystal plate with metal electrodes deposited on each side of the plate. The application of a voltage between the electrodes results in a shear deformation within the quartz crystal due to the piezoelectric properties and crystalline orientation of the quartz [3]. Only those resonant thickness shear modes with maxima displacement at the crystal surface are applied for sensor applications. The high resonance frequency of the QCM makes the device sensitive to its surface perturbation, such as mass absorption. Sauerbery's equation gives the linear relationship between the resonance frequency shift of QCM and mass attached on the electrode surface [4]. This equation and its various refinements generally assume that the mass is uniform and fully attached to the QCM surfaces [4–6]. In many, but not all, cases this is a good approximation. However, the mass and vibration amplitude are not perfectly uniform [7] and the mass loading might be attached on only partial area of the electrode region. Few theoretical studies have been found in literatures on those non-perfect mass attachment problems. In order to be able to make use of the high resolution of QCM measurements, the relation between the frequency changes and the changes of the surface attachment details must be studied.

QCM is operating on its thickness shearing vibration mode. With electrode covering on the quartz crystal, the thickness shearing vibration is trapped on the electrode region because of the energy trapping effect [8]. The vibration amplitude distribution is highly non-uniform within the electrode area. The vibration falls off fast at the electrode edges. Different position of mass deposited on the electrode does have different effect on resonance frequency of the quartz crystal resonator.

In this paper, theoretical studies of a rigid mass partially attached on electrode surface are performed using a model which is based on the Mindlin's theory [9]. With the assumption that the operation frequency is close to the cut-off frequency of the electrode-covering region, the thickness shear mode is decoupled with thickness flexure mode [10]. The performance of the QCM with different percentage of mass attachment area and position of the mass attachment partially mass attachment on electrode surface is analyzed and studied. The resonance frequency is changed with the position of the mass attachment. The numerical simulation results show that QCM with larger electrode size is less sensitive to the percentage of covering area, and QCM with

* Corresponding author. Tel.: +65-6419-1467; fax: +65-6419-1480.
E-mail address: hplee@ihpc.nus.edu.sg (H.P. Lee).

0924-4247/$ – see front matter © 2004 Elsevier B.V. All rights reserved.
doi:10.1016/j.sna.2004.01.018

smaller electrode thickness is less sensitive to the position attachment of the mass absorption on its surface.

2. Model for analysis

The QCM model used for analysis is shown in Fig. 1. It is an infinite AT-cut quartz plate with two electrode layers coated on the top and bottom surfaces. The structure is symmetrical to the *x*-axis. By applying the electrical voltage with a certain frequency on the electrode, thickness shearing vibration will be generated with the electrode-region due to the energy trapping effect. For sensor applications, the mass absorbed on the surface of the electrode will reduce the resonance frequency following the Sauerbery's equation under certain assumptions. The mass absorption maybe occurs on both the top and the bottom surfaces, Small asymmetry effects arising from any mass imbalance between the top electrode surface and bottom surface are neglected.

There are five regions divided for QCM, where mass absorbed partially on the surface of the electrodes. The mass absorbed area is indicated as in Fig. 1 with length D_2, and D_1, D_3 from both edges of electrode. The regions I and V without electrode covering are assumed to be semi-infinite.

2.1. TS and TF coupling motion equations

For the regions with electrode and rigid mass absorption, the coupled vibration equations of TS and TF modes obtained by Mindlin are used here. Neglecting the thickness of mass attached, but taking into account the mass of the surface region III, the motion equation with TS and TF modes can be expressed as [9]

$$c_{66}^{*}k_{6e}^{2}\left(\frac{\partial^2 v}{\partial x^2}+\frac{\partial \psi}{\partial x}\right)=\rho(1+R+R_m)\frac{\partial^2 v}{\partial x^2} \tag{1}$$

$$\gamma_{11}h^2\frac{\partial^2 \psi}{\partial x^2}-3k_{6e}^{2}c_{66}^{*}\left(\frac{\partial v}{\partial x}+\psi\right)+\frac{C}{2h} = \rho h^2(1+3R+3R_m)\frac{\partial^2 \psi}{\partial t^2} \tag{2}$$

where ν and ψ are deflection in *y*-direction and rotation on the line element normal to the mid-plane of the quartz plate, respectively, $c_{66}^{*}=(c_{66}-c_{26}c_{62}/c_{22})+e_{26}^{2}/\in_{22}$ at non-electrode region due to the piezoelectric stiffening effect and $c_{66}^{*}=(c_{66}-c_{26}c_{62}/c_{22})$ at electrode region, is the shearing modulus of the elasticity on *x*–*y* plane, *c* is the mechanically equivalent couple per unit area of the imposed voltage on the electrode, $\gamma_{11}=c_{11}-(c_{12})^2/c_{22}$ is Voigt's stretch modulus of the plate in the *x*-direction, k_{6e}^{2} is the compensate factor which can be calculated from two-dimensional approximate method [9]

$$k_{6e}^{2}=\frac{\pi^2}{12}\frac{(1+3R+3R_m)}{(1+R+R_m)^2} \tag{3}$$

where $R=\rho_e h_e/\rho h$, $R_m=\rho_m h_m/\rho h$, are the ratio of the mass per unit area of electrode and absorption mass to quartz per unit area, ρ_e and ρ_m are densities of electrode material and of absorption mass on surface, h_e and h_m are thickness of electrode and absorption, respectively. At the region where there is no electrode covering, $R=R_m=0$ and $C=0$. The small asymmetric effect arising from mass absorption imbalance on the top and bottom surfaces is neglected in this paper, though the imbalance absorption may occur on the top and bottom surfaces. The structure and vibration are asymmetric to the middle-plane of the quartz plate before and after absorption.

The straight-crested shearing wave is introduced by assuming the line displacement profile in the thickness direction. The shearing displacement can be expressed as:

$$u_x=y\psi \tag{4}$$

Same as the derivation in Ref. [9], the transverse force $Q(x)$ and the bending moment $M(x)$ at the particular position are given as a function of the rotation anger and transverse deflection.

$$Q(x)=2hk_{6e}^{2}c_{66}^{*}\left(\frac{\partial v}{\partial x}+\psi\right) \tag{5}$$

$$M(x)=\frac{2h^3\gamma_{11}}{3}\frac{\partial \psi}{\partial x} \tag{6}$$

When the mass absorption is not on the whole electrode area, the whole QCM structure is divided into five regions (section I–V) as shown in Fig. 1. Considering the energy trapping effect, there are three cut-off frequencies of TS wave expressed as follows:

For regions I and V which are without electrode covering

$$\omega_1^2=\frac{3k_6^2c_{66}^{*}}{\rho h^2} \tag{7}$$

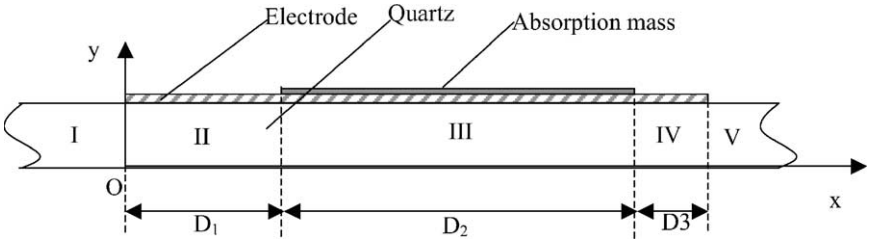

Fig. 1. QCM structure with mass absorption partially attached on surface.

For regions II and IV which are with electrode covering but without mass absorption

$$\omega_2^2 = \frac{3k_6^2 c_{66}^*}{\rho h^2(1+3R)}, \quad k_6^2 = \frac{\pi^2}{12}\frac{(1+3R)}{(1+R)^2} \tag{8}$$

For region III, which is with electrode covering and mass absorption, the cut-off frequency is

$$\omega_3^2 = \frac{3k_6^2 c_{66}^*}{\rho h^2(1+3R+3R_\mathrm{m})}, \quad k_6^2 = \frac{\pi^2}{12}\frac{(1+3R+3R_\mathrm{m})}{(1+R+R_\mathrm{m})^2} \tag{9}$$

2.2. Solutions of decoupling TF and TS modes

Thickness shearing and thickness flexure modes are coupled together in Eqs. (1) and (2). When the disturbance and operation frequency is close to cut-off frequency, $\omega = \omega_2 \pm \Delta\omega$, where $\Delta\omega << \omega_2$, the coupling equations between the TS, and FT modes yields the relation (10).

$$v = -\frac{1}{3}h^2\frac{\partial\psi}{\partial x} \tag{10}$$

Substituting the relation into equations, we obtain a single equation of motions for thickness shearing mode.

$$(\gamma_{11} + k_{6\mathrm{e}}^2 c_{66}^*)h^2\frac{\partial^2\psi}{\partial x^2} - 3k_{6\mathrm{e}}^2 c_{66}^*\psi + \frac{C}{2h} = \rho h^2(1+3R+3R_\mathrm{m})\frac{\partial^2\psi}{\partial t^2} \tag{11}$$

For regions I and V, $R = R_\mathrm{m} = 0$ where it does not have either electrode or attached mass. For regions II and IV, $R_\mathrm{m} = 0$, where it is with electrode covering but without mass absorbed. Eq. (11) is the decoupled TS mode vibration equation. Assuming that a harmonic voltage excitation $C = C_0\,\mathrm{e}^{j\omega t}$ is applied on the electrode surface, harmonic solution for ψ can be expressed as

$$\psi = \varphi\,\mathrm{e}^{j\omega t} \tag{12}$$

Substituting into Eq. (11), the motion equation can be rewritten as

$$\frac{\partial^2\varphi}{\partial x^2} - \xi^2\varphi = -\frac{C}{2h^3(\gamma_{11} + k_{6\mathrm{e}}^2 c_{66}^*)} \tag{13}$$

where

$$\xi_i^2 = \frac{\rho(1+3R+3R_\mathrm{m})(\omega_i^2 - \omega^2)}{\gamma_{11} + k_6^2 c_{66}^*} \qquad i = 1\text{–}3,$$

for three types of region.

When the operating frequency is assumed for the range, $\omega_1 \geq \omega \geq \omega_2 \geq \omega_2$, the thickness shearing wave will attenuate exponentially at regions I and V, and it can be propagated in regions II–IV due to the energy trapping effect. When a electrical voltage mechanically equivalent to $C = C_0\cos(\omega t)$ is impressed across the electrode, the solution of Eq. (13) includes transient response and steady-state response. The transient response of the constant C_0 is not involved in the resonance characteristics analysis. The steady-state response of the electrode region is the sum of the external impressed equivalent force and its harmonic response. With arbitrary constants a_i, $i = 1$–8, the harmonic solutions of rotation in each of the regions I–IV can be written as

$$\varphi_1 = a_1\exp(\xi_1 x_1) \quad x_1 \leq 0 \quad \text{region I} \tag{14}$$

$$\varphi_2 = \varphi_0^{(2)} + a_2\cos(\xi_2 x_1) + a_3\sin(\xi_2 x_1) \quad 0 \leq x_1 \leq D_1 \quad \text{region II} \tag{15}$$

$$\varphi_3 = \varphi_0^{(3)} + a_4\cos(\xi_3 x_1) + a_5\sin(\xi_3 x_1) \quad D_1 \leq x_1 \leq D_1 + D_2 \quad \text{region III} \tag{16}$$

$$\varphi_4 = \varphi_0^{(2)} + a_6\cos(\xi_2 x_1) + a_7\sin(\xi_2 x_1) \quad D_1 + D_2 \leq x_1 \leq D_1 + D_2 + D_3 \quad \text{region IV} \tag{17}$$

$$\varphi_5 = a_8\exp(-\xi_1 x_1) \quad D_1 + D_2 + D_3 \leq x_1 \quad \text{region V} \tag{18}$$

where

$$\varphi_0^{(2)} = \frac{C_0}{2h^3\rho(1+3R)(\omega_2^2 - \omega^2)}$$

$$\varphi_0^{(3)} = \frac{C_0}{2h^3\rho(1+3R+3R_\mathrm{m})(\omega_3^2 - \omega^2)}$$

The conditions of continuity of displacement and moment at the boundaries of different regions of the plates requires that

$$\varphi_i = \varphi_{i+1} \tag{19}$$

$$\frac{\partial\varphi_i}{\partial x} = \frac{\partial\varphi_{i+1}}{\partial x} \tag{20}$$

at $x = 0$, $x = D_1$, $x = D_1 + D_2$ and $x = D_1 + D_2 + D_3$. These continuity conditions providing eight equations for constants a_i, $i = 1$–8, which can be obtained.

$$[M]_{8\times8}\{a\}_{8\times1} = \{\varphi_0\}_{8\times1} \tag{21}$$

Table 1
Material properties of AT-cut quartz and silver electrode of QCM

AT-cut quartz	Silver electrode
Density (kg/m^3) $\rho = 2675$	$\rho_\mathrm{e} = 10,500$
Stiffness modulus (GPa) $c_{11} = c_{22} = 86.74$, $c_{12} = 6.99$, $c_{66} = 62.51$, $c_{26} = c_{62} = 0$	Voigt's stretch modulus (GPa) $\gamma_{11} = c_{11} - (c_{12})^2/c_{22} = 86.177$
Thickness $h = 0.2$ mm	$h_\mathrm{e} = 300$ nm

where

$$\begin{bmatrix} 1 & -1 & 0 & 0 & 0 & 0 & 0 & 0 \\ \xi_1 & 0 & -\xi_2 & 0 & 0 & 0 & 0 & 0 \\ 0 & b_{21} & s_{21} & -b_{31} & -s_{31} & 0 & 0 & 0 \\ 0 & -\xi_2 s_{21} & \xi_2 b_{21} & \xi_3 s_{31} & -\xi_3 b_{31} & 0 & 0 & 0 \\ 0 & 0 & 0 & b_{32} & s_{32} & -b_{22} & -s_{22} & 0 \\ 0 & 0 & 0 & -\xi_3 s_{32} & \xi_{32} b_{32} & \xi_2 s_{22} & -\xi_2 b_{22} & 0 \\ 0 & 0 & 0 & 0 & 0 & b_{23} & s_{23} & -\mathrm{e}^{-\xi_1 d_3} \\ 0 & 0 & 0 & 0 & 0 & -\xi_2 s_{23} & \xi_2 b_{23} & \xi_1 \mathrm{e}^{-\xi_1 d_3} \end{bmatrix} \begin{Bmatrix} a_1 \\ a_2 \\ a_3 \\ a_4 \\ a_5 \\ a_6 \\ a_7 \\ a_8 \end{Bmatrix} = \begin{Bmatrix} \varphi_0^{(2)} \\ 0 \\ \varphi_0^{(3)} - \varphi_0^{(2)} \\ 0 \\ \varphi_0^{(2)} - \varphi_0^{(3)} \\ 0 \\ -\varphi_0^{(2)} \\ 0 \end{Bmatrix}$$

where

$$b_{ij} = \cos(\xi_i d_j)\, s_{ij} = \sin(\xi_i d_j), \quad i = 1\text{–}3, \quad j = 1\text{–}3$$

$$d_j = D_1,\ D_1 + D_2,\ D_1 + D_2 + D_3$$

To satisfy the equations, the resonance condition requires the determinant of the coefficient matrix $[M]_{8\times 8}$ to be zero. The determinant of the matrix is a function of the electrode length and parameters of the mass attached on the electrode surface.

3. Numerical simulation and results

In this section, simulations for QCM with partially attached mass on surface are performed. With materials properties of AT-cut quartz crystal and silver electrode on surfaces as shown in Fig. 1, the effect of the size and position of the attached mass are analyzed and discussed. The thickness of the quartz and dimensions of electrode are also listed in Table 1.

3.1. Mass absorption uniformly covering whole electrode area

With different electrode size, the resonance frequency of the first TS mode is different. The resonance spectrum of the QCM with different electrode size is shown in Fig. 2. The resonance frequency of TS mode approaches that of cut-off frequency with increasing electrode size.

For sensor applications of QCM, the resonance frequency shift of the first TS mode is a function of the mass attached on quartz surface. The normal expression of the mass sensitivity is expressed as

$$\frac{\Delta f}{f} \doteq -\frac{\Delta R_\mathrm{m}}{1 + R + R_\mathrm{m}} \tag{22}$$

in which, the frequency sensitivity of QCM is independent on the electrode size. However, from the dispersion relations, it can be seen that the resonance frequency of QCM relates to the electrode area. This effect is not only due to the coupling of TF and TS vibration mode as mentioned in Ref. [11], in which the relationship between the frequency shift is expressed as a function of the absorption mass in unit area. Even with decoupling of TF and TS modes used in this paper, the sensitivity of QCM also decreases as the electrode size decreases. As similarly shown in Fig. 3, the simulation is performed with mass absorption fully attached on the electrode surface, i.e. $D_1 = D_3 = 0$, and the sensitivity with different electrode size is calculated. The difference between the calculated sensitivity of QCM and nominal sensitivity is enlarged as the electrode size

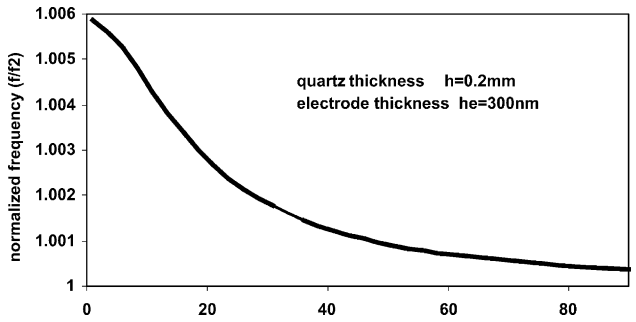

Fig. 2. TS mode resonance frequency spectrum of QCM without absorption.

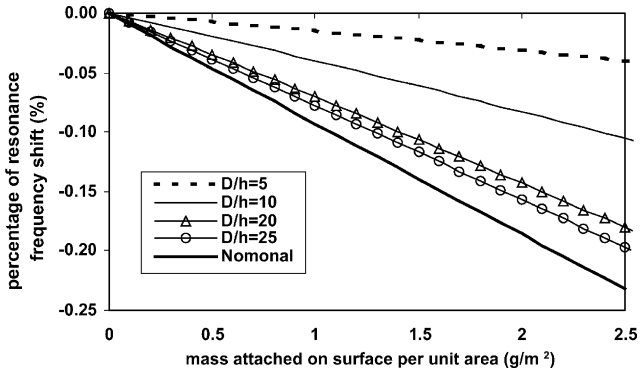

Fig. 3. Frequency sensitivity of QCM as a function of mass absorption unit area with different size of electrode size.

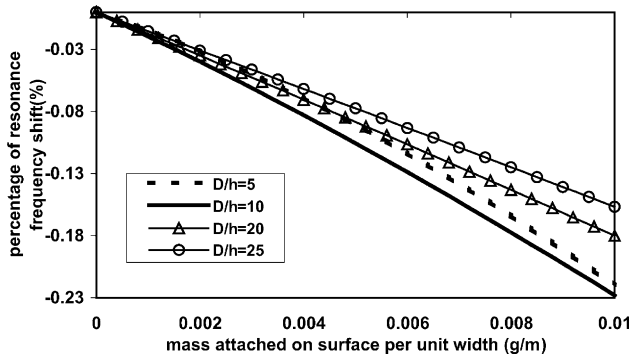

Fig. 4. Frequency sensitivity of QCM as function of mass absorption per unit width with different size of electrode size.

decreases. This can be explained that the total mass attached on the electrode surface is reduced with decreased electrode size having the same absorption mass thickness. If we keep the mass constant, the similar figure plot as a function of total absorption mass on the surface, this trend as indicated in Fig. 4 is different from Fig. 3. Since the QCM is mostly used to detect the thickness of absorption, larger electrode size provided higher sensitivity to thickness of absorption mass.

3.2. QCM with mass absorption partially on the surface

From the vibration profile of the QCM as shown in Fig. 5, it can be seen that the amplitude of the TS vibration decreases very fast as close to the edges of the electrode. When the absorption mass is not fully attached on the electrode surface, the percentage of the covering will affect the TS resonance frequency shift.

Under the condition of symmetric distribution of the absorption mass on electrode surface, i.e. $D_1 = D_3$, Fig. 6 gives the TS resonance frequency shift with different percentage covering of absorption mass on the electrode surface with different mass absorption volume.

When the covering area decreases, the absorption mass is concentrated at the center of the electrode where the vibration amplitude is lager than that of the electrode edge. The resonance frequency of TS mode is decreased when the absorption area is decreased as shown in Fig. 6 even with the same volume of the absorption mass. The difference between 30% covering and full covering can be several kilohertz. Fig. 7 presents the comparison of this covering area effect for different electrode sizes. Keeping the mass volume constant as increasing the absorption percentage from 30 to 100% of the electrode length, the resonance frequency shift value for

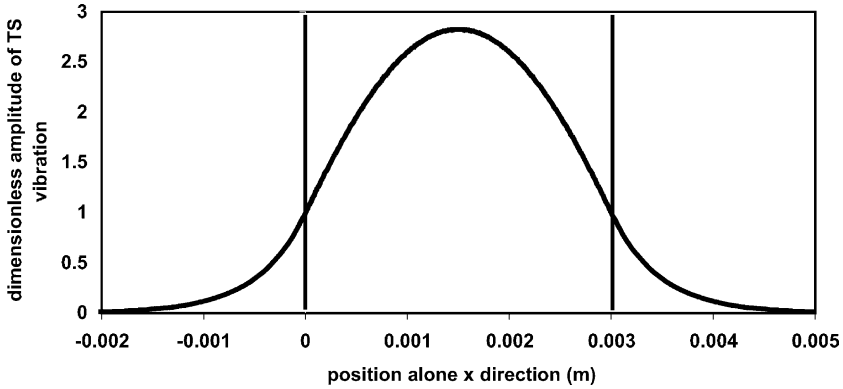

Fig. 5. TS vibration profile alone *x*-direction.

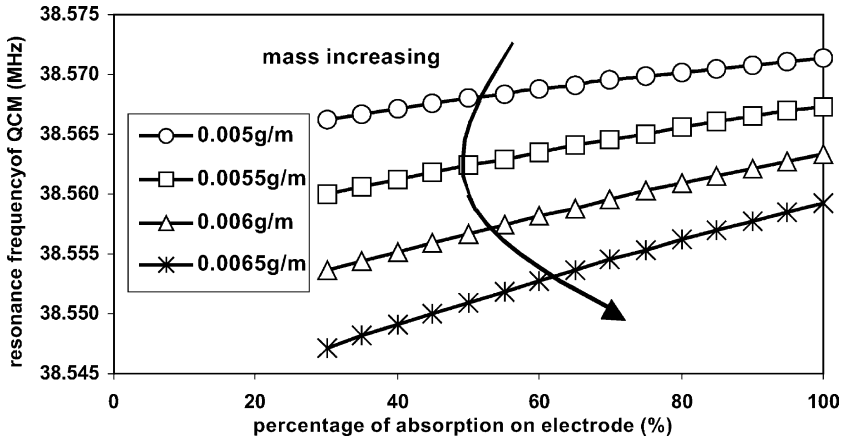

Fig. 6. TS resonance of QCM as a function of percentage covering area of mass absorption (with constant mass and electrode length $D/h = 15$).

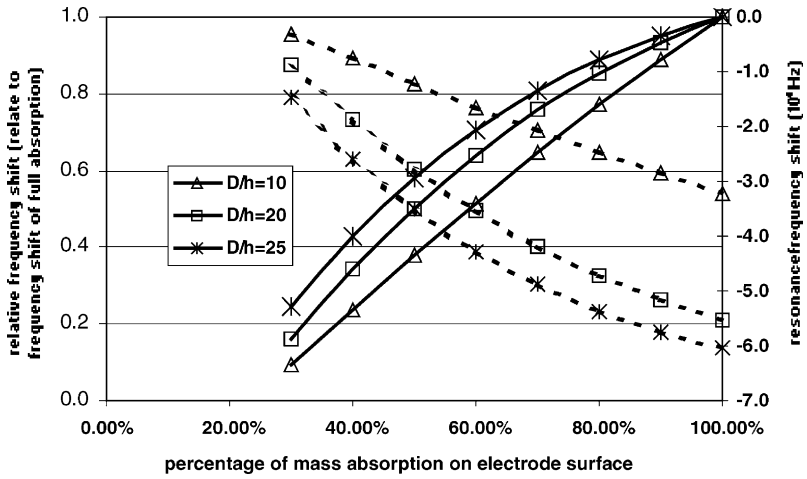

Fig. 7. Covering area effect of the absorption mass for different electrode length (solid line: relative shift comparing with frequency shift of full covering; dot line: absolute frequency shift).

different QCMs with different electrode length ($D/h = 10$, 20, 25, respectively) are shown as dotted lines. The relative frequency shift (relate to frequency shift of full absorption) due to the difference of the absorption position is shown as solid lines. From the solid lines, it can be seen that with an increase of the electrode size, this covering area effect of absorption mass is less significant as shown in Fig. 7.

With partially absorption mass on the surface, there is a chance for mode jump, since the cut-off frequency of TS mode in absorption region is less than that of the other electrode regions. When the thickness of the absorption reaches a certain value, the TS resonance frequency QCM will be smaller than the cut-off frequency of a naked electrode region ω_2. The main TS vibration will be trapped within the absorption mass region.

3.3. Effect of position of the absorption mass on the electrode surface

Keeping the attachment mass constant, and the attachment position moving from electrode edge to center, the resonance frequency of the QCM decreases. This frequency shift is not due to the different mass volume, but due to the different mass position. Fig. 8 gives the resonance frequency shift with different mass attachment area moving from edge to center of the electrode. It is shown that the resonance frequency of QCM is decreased as the constant mass moves from electrode edge to center position. Three cases are analyzed with the same mass volume as shown in Fig. 8, i.e. 40, 50 and 60% covering area, respectively. It is shown that with smaller attachment area, the effect of the different attachment position is more significant.

Keeping the same thickness and percentage of attachment area of the absorption on electrode surface, Fig. 9 shows the effect of the electrode thickness and electrode length to the position sensitivity. The maximum difference of resonance frequency due to the attached position is calculated as functions of the electrode length (length/thickness ratio). The maximum difference of resonance frequency due to position of mass absorbed is expressed as

$$\Delta f_{\mathrm{m}} = f_{\mathrm{edge}} - f_{\mathrm{center}} \tag{23}$$

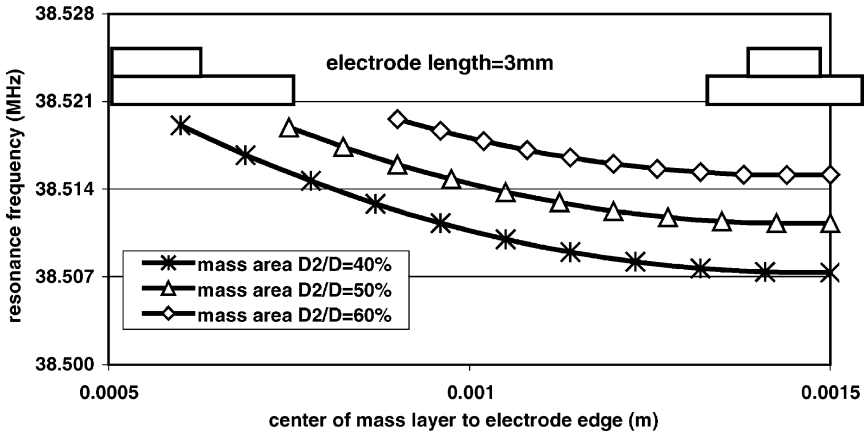

Fig. 8. Resonance frequency shift due to the different position of absorption from edge position to center of the electrode (absorption mass per unit width = 0.01 g/m).

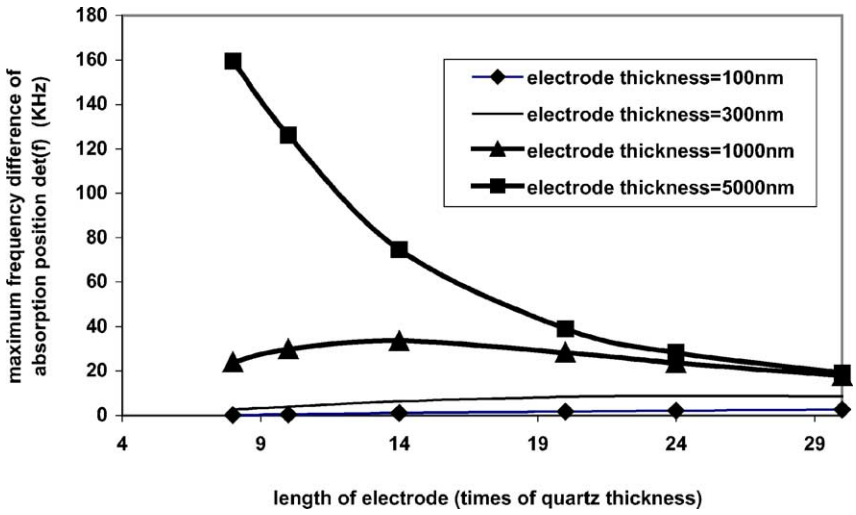

Fig. 9. The maximum frequency difference with absorption mass moving from edge to center as function of electrode length for different electrode thickness. The mass absorption is set to be 50% of electrode length, and the mass volume per unit width for each electrode thickness is kept constant mass = 0.005 g/m.

where f_{edge} and f_{center} are resonance frequencies of compounded QCM when mass absorbed on edge of electrode and that of QCM when mass absorbed on center of QCM. The larger Δf indicates the more significant mass position dependence for QCM.

It is found that the significance of the absorption position effect on compounded QCM is related to the thickness of electrode. The position sensitivity of QCM with electrode thickness 100 nm is lowest and even appears to be independent of the electrode length. It implies that QCM with thin electrode results in a more constant resonance frequency with different absorption mass for compounded QCM. And thinner electrode can be the chose for sensor applications to reduce the position dependence of the resonance frequency of compounded QCM.

Thicker electrode layer on quartz surface can be used to increase the energy trapping effect of QCM, so as to increase the Q-factor or reduce the coupling between adjacent QCM for multi-channel QCMs applications. The energy trapping effect of the thickness shearing vibration of quartz plate is significant with a thick electrode etched on the surface, as the vibration amplitude will drop faster at the edge. For that case, a larger electrode size results in a more constant resonance frequency with different absorption positions and gives more accurate results of mass attached despite the mass absorption position as shown in Fig. 9.

4. Conclusion

An AT-cut Quartz crystal microbalance with absorption mass partially attached on surface is analyzed using Mindlin's plate theory. Because of the energy trapping effect, amplitude of the vibration of the thickness shearing mode is different on the QCM surface. With mass absorption on different position of the electrode surface, the induced resonance frequency shift is different. In this paper, the effect of the percentage of the covering area and position of the absorption mass is analyzed and discussed. The numerical simulation shows that QCM with a thinner electrode is better to reduce the effect of the partial absorption of the mass attachment, and so will result in a more accurate measurement results for sensor applications.

References

[1] C. Lu, A.W. Czanderna Applications of Piezoelectric Quartz Crystal Microbalances, Elsevier, Amsterdam, 1984.
[2] A. Janshoff, H.J. Galla, C. Steinem, Piezoelectric Mass-Sensing Devices as Biosensors—An Alternative to Optical Biosensors, Angewandte Chemie International Edition, vol. 39, 2000, pp. 4004–4032.
[3] D.S Ballantine Jr., R.M. White, S.J. Martin, A.J. Ricco, G.C. Frye, E.T. Zellers, H. Wohltjen, Acoustic Wave Sensors: Theory, Design and Physico-Chemical Application, Academic Press, 1997.
[4] G. Sauerbery, Verwendung Von Schwingquarzen Zur Wagung Dunner Schechten and Zur Mikrowagung, Z. Phys. 155 (1959) 206–222.
[5] C.S. Lu, O. Lewis, Investigation of film-thickness determination by oscillating quartz resonators with large mass load, J. Appl. Phys. 43 (11) (1972) 4385–4390.
[6] C.E. Reed, K. Keiji Kanazawa, J.H. Kaufman, Physical description of a viscoelastically loaded AT-cut quartz resonator, J. Appl. Phys. 68 (5) (1990) 1993–2001.
[7] R. John Vig, A. Ballato, Comments about the effects of nonuniform mass loading on a quartz crystal microbalance, IEEE Trans. UFFC 45 (5) (1998) 1123–1124.
[8] K. Hirama, Y. Aoyama, R. Yasuike, K. Yamazaki, Trapped-energy AT-cut quartz crystal units with grooves, in: IEEE International Frequency Control Symposium, 1997, pp. 750–757.
[9] R. D Mindlin, P.C.Y. Lee, Thickness-shear and flexural vibrations of partially plated crystal plates, Int. J. Solids Struct. 2 (1966) 125–139.
[10] J. Zelenka, Piezoelectric Resonators and the Applications, Elsevier, 1986.
[11] K.H. Lee, F. Shen, P. Lu, S.J. O'Shea, T.Y. Ng, Frequency interference between two quartz crystal microbalance, in: The First IEEE International Conference on Sensors Orlando, Florida, USA, 11 June 2002, pp. 1148–1153.

Biographies

Feng Lu was born in Jiangsu, PR China, 1974. He obtained his bachelor and master degree in Department of Mechanics Engineering, Xi'an Jiaotong University, PR China 1996 and 1999, respectively. He worked as R&D engineer in the Philips Electronics Company Singapore before he became a PhD candidate in National University of Singapore in January 2002. His current research interests are in acoustic wave biosensors and piezoelectric actuators.

H.P. Lee is currently the acting executive director of the Institute of High Performance Computing (IHPC) as well as an associate professor at the Department of Mechanical Engineering, National University of Singapore. He has held position as the sub-dean for external relations in the Faculty of Engineering, National University of Singapore as well as the Deputy Executive Director for Research at IHPC. He obtained his PhD and MS from the Department of Mechanical Engineering, Stanford University, BA from the University of Cambridge. His research interests are in the areas of vibration and acoustics, computational mechanics, numerical methods, and computational MEMS.

S.P. Lim is currently the deputy head of the Applied Mechanics Division of the Department of Mechanical Engineering, National University of Singapore. He obtained his PhD from the University of Southampton. His research interests are in the areas of vibration and acoustics, computational mechanics, numerical methods, computational MEMS, and electrophoresis.